

ZrSiO₄ Oxidation Protective Coating for SiC-Coated Carbon/Carbon Composites Prepared by Supersonic Plasma Spraying

Can Sun, He-jun Li, Qian-gang Fu, Hai-liang Li, Yong-jie Wang, and Heng Wu

(Submitted May 13, 2012; in revised form February 18, 2013)

To protect carbon/carbon (C/C) composites against oxidation, ZrSiO₄ oxidation protective coating was prepared on SiC-coated C/C composites by supersonic plasma spraying. X-ray diffraction and scanning electron microscopy were used to analyze the phase and microstructure of the coating. The results show that the as-prepared ZrSiO₄ coating is continuous and well bonded with the SiC inner layer without penetrating crack, which exhibits good oxidation-resistant properties. After oxidation at 1773 K in air for 97 h and nine thermal shock cycles between 1773 K and room temperature, the weight loss of the coated C/C composites was only 0.08%. The excellent oxidation-resistant properties of the coating were attributed to its dense structure and the formation of the stable ZrO₂-SiO₂ glassy mixture on the surface of ZrSiO₄ coating.

Keywords carbon/carbon composites, oxidation, SiO₂, ZrO₂ oxidation, ZrSiO₄ coating

1. Introduction

Carbon/carbon (C/C) composites have attracted wide attention in aircraft and aerospace fields because of their excellent mechanical properties under high temperature (Ref 1), such as high strength-to-weight ratio and high retention of mechanical properties at high temperatures (Ref 2, 3). However, these composites tend to be oxidized during their exposure to an oxidizing atmosphere above 723 K (Ref 4). The oxidation results in an obvious decrease of the mechanical properties, which limits their performances as high-temperature structural materials.

To improve the oxidation resistance property of C/C composites, different kinds of ceramic coating systems, such as C/SiC, yttrium silicate, ZrO₂-CaO-ZrSiO₄, ZrO₂-Y₂O₃-ZrSiO₄, and MoSi₂-SiC-Si/SiC/borosilicate glass coating have been developed (Ref 5-8). ZrB₂-MoSi₂/SiC (Ref 9) gradient multilayer coating by slurry painting exhibited good oxidation resistance at 1773 K. The cracks in the coating possessed self-sealing performance due to the formation of ZrSiO₄ and SiO₂ glaze during the oxidation process. However, the coating prepared by slurry painting showed low adhesive strength and uneven dis-

tribution of composition that influenced its application at high temperature for long time.

As one of silicates, ZrSiO₄ possesses high stability in oxidative and corrosive environments, low thermal expansion, low thermal conductivity, as well as good corrosion resistance (Ref 10). Moreover, slurry painting and in situ reaction techniques also have been used to obtain ZrSiO₄ outer coatings, but the low bonding strength between the ZrSiO₄ coatings and the inner coatings limits their application (Ref 11). Supersonic plasma spraying with plasma temperature in the region of 10,000 K and in jet velocities of up to 600 m/s is a novel method to prepare coating. The powders are carried and delivered into the plasma jet by gas. After being melted and accelerated, the powders impinge on the substrate to form a compact coating (Ref 12, 13). Currently some coating systems, such as MoSi₂-based ceramics, mullite, and yttrium silicate (Ref 14, 15), have been prepared by this method, which creates good properties for protecting C/C composites. Up to now, little has been reported on preparing ZrSiO₄ coatings for C/C composites by the supersonic plasma spraying technique.

In the present work, supersonic plasma spraying was used to prepare ZrSiO₄ coating on the surface of SiC-coated C/C (SiC-C/C) composites. The microstructures and high-temperature oxidation resistance of ZrSiO₄ coating were investigated.

2. Experimental

Specimens (15 × 5 × 5 mm) used as the substrates were cut from bulk 2D C/C composites with a density of 1.75 g/cm³. These specimens were abraded by using 80 and 300 grit SiC paper in turns, then cleaned ultrasonically in acetone and dried at 393 K for 1-2 h. Prior to the preparation of outer ZrSiO₄ coating by supersonic plasma spraying, the SiC inner coating was prepared by a pack

Can Sun, He-jun Li, Qian-gang Fu, Hai-liang Li, Yong-jie Wang, and Heng Wu, State Key Laboratory of Solidification Processing, Northwestern Polytechnical University, Xi'an 710072, People's Republic of China. Contact e-mails: suncan7@gmail.com and lihejun@nwpu.edu.cn.

cementation process with Si, C, and $\text{Al}_2\text{O}_3/\text{B}_2\text{O}_3$ mixed powders in an argon atmosphere at 1973–2173 K for 2 h. The details of preparing SiC transition layer by pack cementation are reported elsewhere (Ref 16, 17).

The ZrSiO_4 powder (Zibo Tonbon Zirconium Industry Co., Ltd.) has a particle size of 50–75 μm , and purity is more than 98 wt.%. The spraying system consists of plasma torch, powder feeder, gas supply, water-cooling circulator, and control unit with PC interface and power supply unit. The spraying parameters are listed in Table 1. With the heating rate of 4 K/min in air, the coated C/C specimens were tested at 1773 K in an electrical furnace to investigate the isothermal and thermal cycling oxidation behavior. X-ray diffractometer (XRD, Rigaku D/max-3C) with a Cu $\text{K}\alpha$ ($\lambda = 0.1542 \text{ nm}$) radiation was used to analyze the phase composition of ZrSiO_4 coating. The analyzed range of the diffraction angle 2θ was between 10° and 85° with a step width of 0.033° . The morphology and crystalline structure of the ZrSiO_4 -based coatings were analyzed by scanning electron microscopy (SEM; EDS, Supra 55).

3. Results and Discussion

3.1 Microstructure of the Coatings

Figure 1 shows an x-ray pattern and SEM surface morphology of coating obtained by pack cementation process. The coating consisted of free silicon, β -SiC, and α -SiC (Fig. 1a). The thermal mismatch between C/C and

Table 1 Details of the spraying parameters for the ZrSiO_4 coatings

Spraying voltage, V	400–420
Spraying current, A	115–140
Primary gas (Ar) flow rate, m^3/h	7.9–8.4
Secondary gas (H_2) flow rate, m^3/h	1.0–1.4
Carrier gas (Ar) flow rate, m^3/h	0.016–0.024
Powder feed rate, g/min	~25
Spraying distance, mm	100
Nozzle diameter, mm	5.5

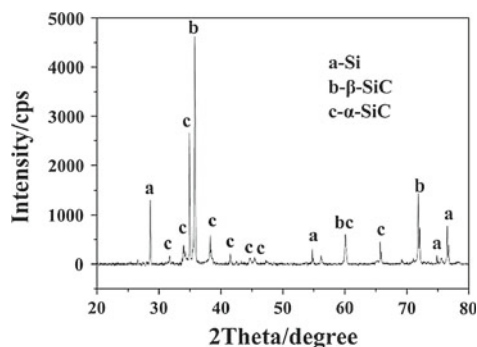
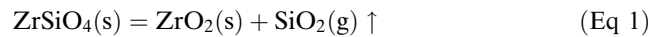


Fig. 1 X-ray patterns and SEM micrograph of the surface of the SiC-coated C/C composites. (a) XRD pattern of SiC coating. (b) SEM micrograph on the surface of SiC coating

the coating can be relaxed by the existence of free silicon (Ref 18). However, the cracking of SiC coating is unavoidable (Ref 19, 20); some cracks are shown in Fig. 1(b). Therefore, the monolayer SiC coating may not provide an excellent oxidation protective ability as a result of the formation of some cracks, through which oxygen could immerse into C/C substrate.

Figure 2 presents the surface XRD of the ZrSiO_4 coating obtained from the supersonic plasma spraying. It reveals that the phase composition of the coating was ZrSiO_4 and ZrO_2 . During supersonic plasma spraying, with the temperature of plasma arc above 3000 K, ZrSiO_4 powder melted rapidly and some of the particles may be decomposed according to:



To illustrate the foregoing analysis better, Gibbs free energy (ΔG) and absorbed heat (ΔH) of the reactions were introduced, which were also calculated by FactSage software (one of the largest fully integrated database computing systems in chemical thermodynamics). The results are listed in Table 2.

As indicated by Table 2, the Gibbs free energy of the decomposition reaction (Eq 1) was -1.4047 kJ/mol at

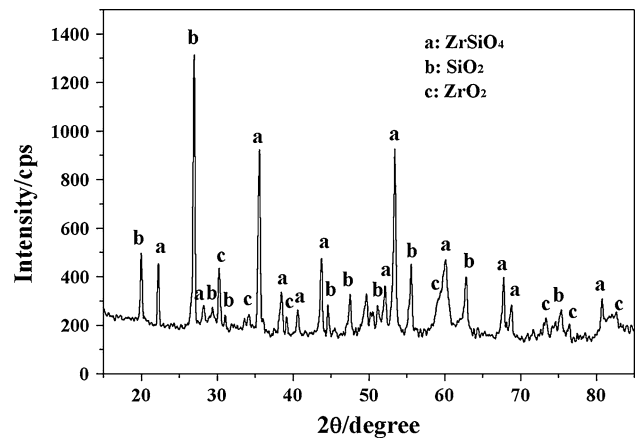
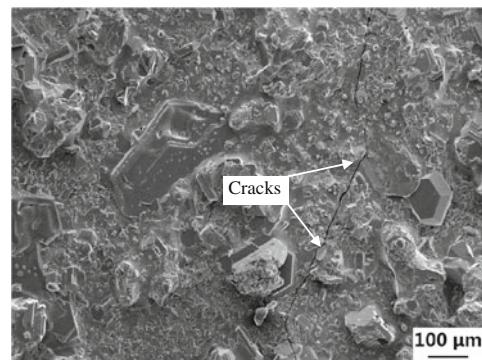


Fig. 2 XRD patterns of ZrSiO_4 coating



1900 K, and the value of ΔG continued to decrease when the temperature increased. As a result, the reaction (Eq 1) was spontaneous because of the negative value of ΔG . According to the surface EDS analyses of ZrSiO_4 coatings, the O, Si, and Zr element content in the coatings was 67, 16, and 17 at.%, respectively. With the combination of XRD patterns (Fig. 2) and EDS, the mole percentage of ZrSiO_4 and ZrO_2 calculated by law of conservation of mass was about 94 and 6%, respectively.

Figure 3 shows the morphology features of ZrSiO_4 -based coating after supersonic plasma spraying. The ZrSiO_4 coating (Fig. 3a) was dense without obvious cracks. From the magnified image (Fig. 3b), it can be seen that some pores existed in the surface of coating, which was attributed to the rapid condensation of molten ZrSiO_4 powder during plasma spraying. According to Fig. 3(c), the outer coating ZrSiO_4 presented a uniform thickness of

Table 2 Changes in Gibbs free energy and absorbed heat of decomposition reactions of ZrSiO_4

Temperature (T), K	Gibbs free energy (ΔG), kJ/mol	Absorbed heat (ΔH), kJ/mol
ZrSiO_4 (s) = ZrO_2 (s) + SiO_2 (s) 1900	-1.4047	28.7
ZrSiO_4 (s) = ZrO_2 (s) + SiO_2 (g) 3545	-61.4894	678.0987

around 150-200 μm without penetrating cracks. In addition, the interface of ZrSiO_4 -SiC coatings was combined mechanically without defects, indicating a good bonding between the inner and outer coatings.

3.2 Oxidation Protective Ability of the Coating

The results of the isothermal oxidation tests in air at 1773 K are shown in Fig. 4. After oxidation for 20 h in air

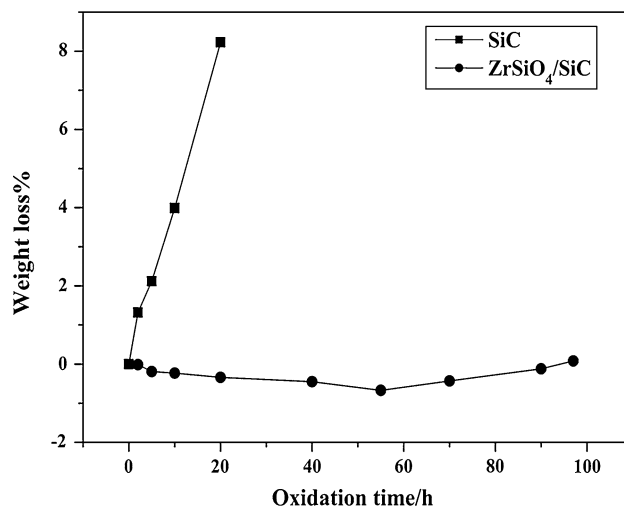


Fig. 4 Oxidation curves of the coated C/C composites at 1773 K in air

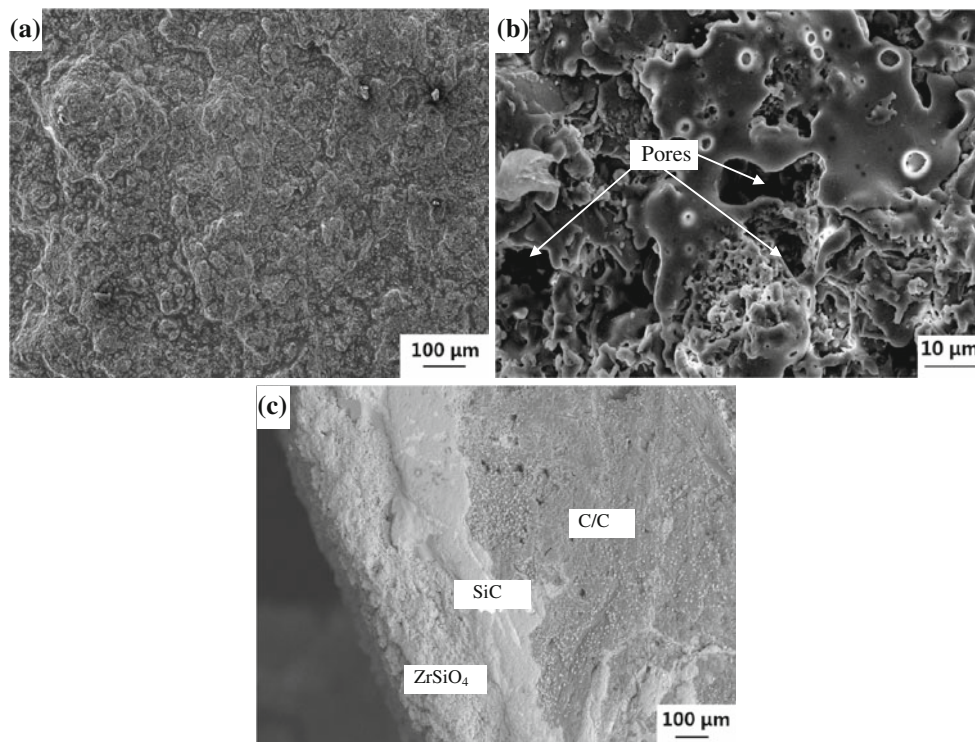


Fig. 3 SEM micrographs of the ZrSiO_4 -based coating. (a) Surface morphology. (b) Magnified image of surface morphology. (c) Cross-section morphology of the ZrSiO_4 -based coating

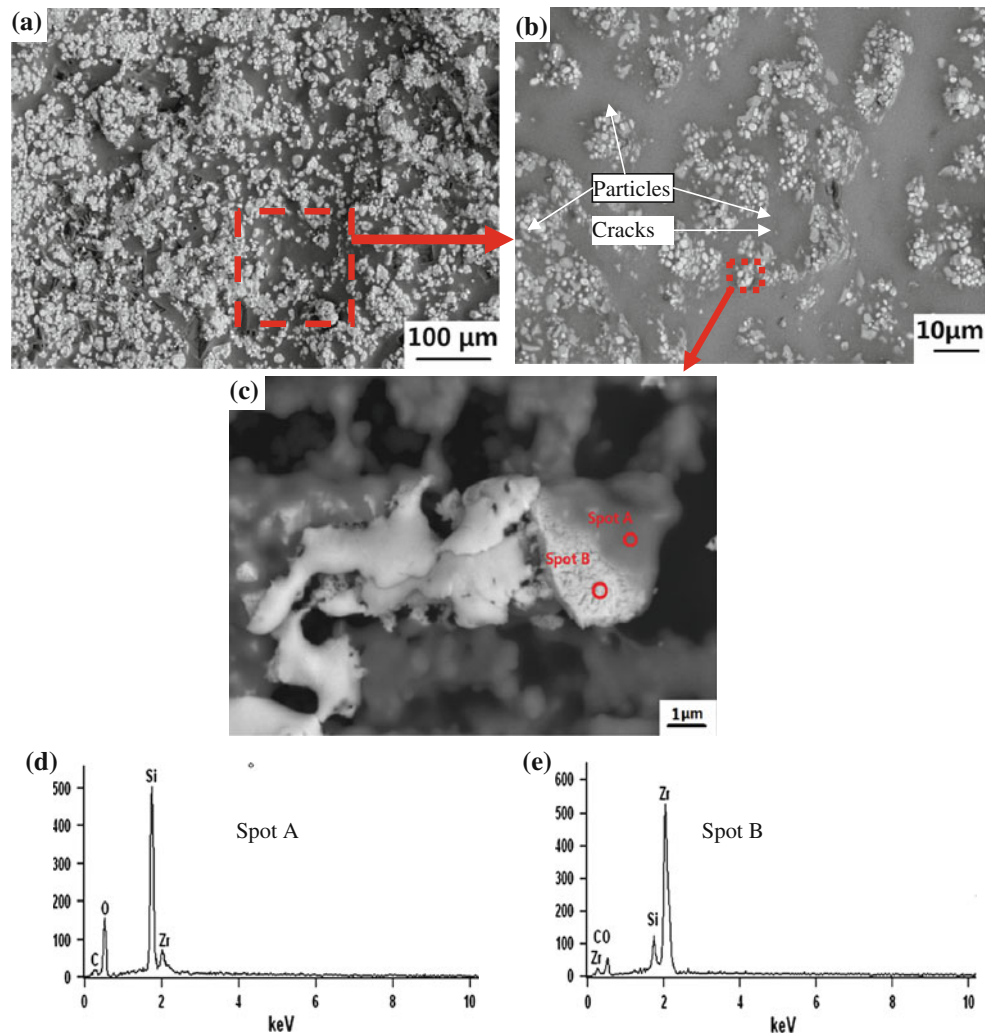
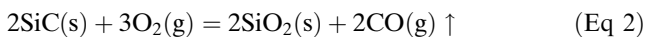


Fig. 5 Micrograph and the spot EDS analyses of the surface of $ZrSiO_4$ coatings after oxidation for 55 h. (a) Surface morphology. (b) Magnification of local region. (c) Local amplification of ceramic particle. (d) and (e) Spot EDS analyses

at 1773 K, the SiC-C/C composites lost its weight of 8.26% as a result of the porous structure of SiC coating. Under the same conditions, the $ZrSiO_4$ -coated SiC-C/C composites prepared by supersonic plasma spraying has almost no weight loss in 8 h and lost only 0.08% mass in 97 h with exposure to air at 1773 K. The $ZrSiO_4$ -SiC coating exhibits better oxidation resistance properties than those of the SiC monolayer coating.

From the oxidation curve (shown in Fig. 4), the oxidation behavior of $ZrSiO_4$ /SiC coated C/C composites can be divided into two segments including weight gain and weight loss. At the first stage of oxidation (less than 55 h), some part of $ZrSiO_4$ (because of its low purity) decomposed to SiO_2 and ZrO_2 (Ref 21). In addition, a small amount of oxygen might diffuse through micropores in the $ZrSiO_4$ outer layer, resulting in the oxidation of SiC inner coating (Ref 22):



In this stage, the weight gain of the coating can be attributed to the oxidation of SiC. After oxidation in air

for 55 h, the weight gain of the coating reached to 0.67%. With the increase of oxidation time, the coating started to exhibit the trend of weight loss, which might be attributed to the consumption of SiO_2 glass or even the oxidation of C/C composites.

Figure 5(a) shows the backscattered electron images (BEI) of the surface of coating after oxidation at 1773 K in air for 55 h. Many white fine ceramic particles are distributed on the surface of the outerwear coating. The microstructure with a larger magnification in the web region is shown in Fig. 5(b). It can be seen that a smooth glassy film with dispersed glassy mixture particles embedded in the surface of the coating. The cracks were surrounded by that particles, and they did not continue to extend along the surface of coating; instead, they were blocked by the glassy mixture particles.

Figure 5(c) is a larger magnification of the web region in Fig. 5(b), enhancing the glassy mixture particles. Figure 5(c) clearly shows that there were two kinds of crystalline particles; they are marked as Spot A and Spot

B on the coating. Spot EDS analysis (Fig. 5d, e) found the composed elements of the gray phase Spot A to be mainly O and Si, while those of the white phase Spot B were mainly Si, O, and Zr. Addition of the XRD analysis in Fig. 6 shows that the gray phase Spot A was composed of SiO_2 and the white phases were composed of ZrSiO_4 and ZrO_2 . From Fig. 5(c), it can be observed that the ZrSiO_4 and ZrO_2 particle were enveloped by glassy SiO_2 forming glassy mixture attached tightly to the material, which can eliminate the porosity of outer coating and restrain the volatilization of SiO_2 effectively. According to the binary

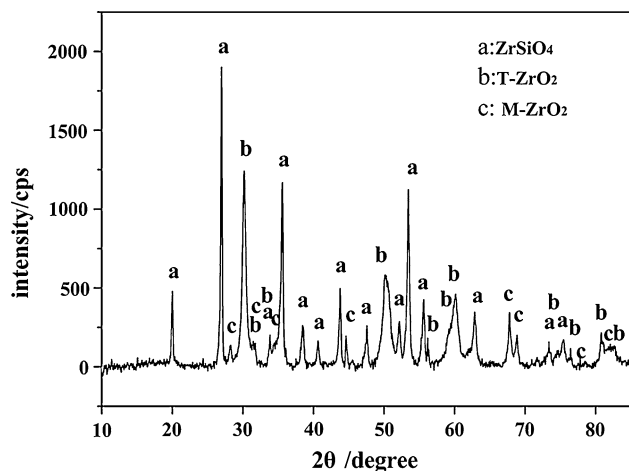


Fig. 6 XRD pattern of $\text{ZrSiO}_4/\text{SiC}$ coating after oxidation

phase diagram of $\text{ZrO}_2\text{-SiO}_2$ (Fig. 7), ZrSiO_4 and ZrO_2 mixture phases are formed by the eutectic reaction between ZrO_2 and SiO_2 during high-temperature exposure (Ref 9, 21). Furthermore, in the SiO_2 -rich phase, the ZrO_2 particles were entirely embedded in newly formed zircon aggregates with interconnecting sinter necks, thus creating a new structure.

In the second stage (after 55 h), ZrSiO_4 continued to decompose into SiO_2 and ZrO_2 . SiO_2 was able to fill in the pinholes in outer coating because of its extremely low oxygen permeation constant (Ref 18). However, long

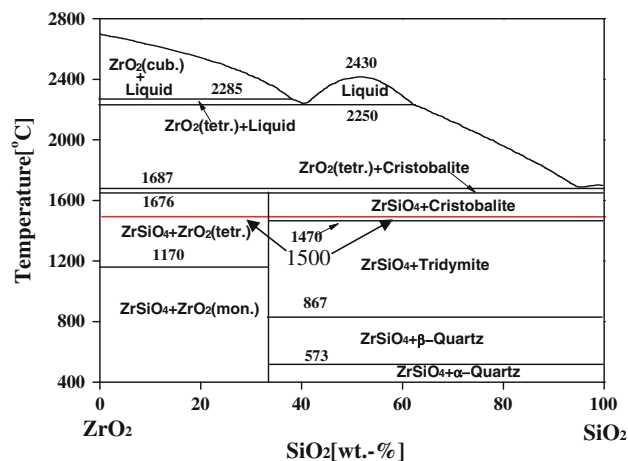


Fig. 7 Phase diagram of $\text{ZrO}_2\text{-SiO}_2$ (22)

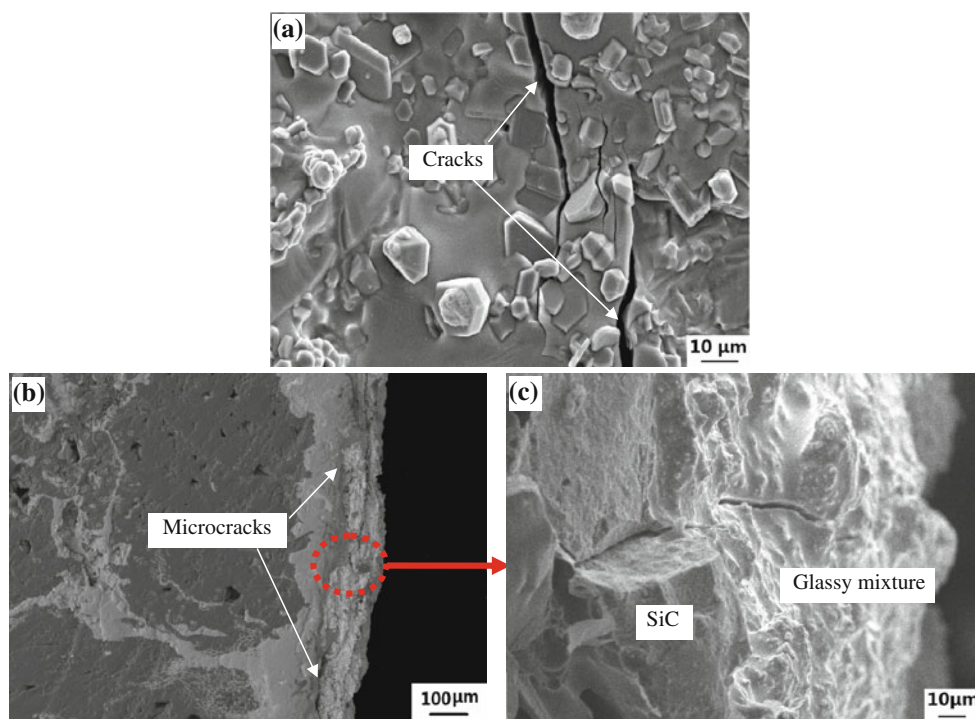


Fig. 8 SEM images of the ZrSiO_4 coatings after oxidation for 97 h. (a) Surface morphology. (b) Cross-section micrograph of the coated C/C composites. (c) Magnification of cross-section micrograph of the coating

service at the experiment temperature would result in the failure of the coating as a result of the volatilization of SiO₂.

Figure 8 shows the SEM microstructure of the sample after oxidation at 1773 K in air for 97 h. From Fig. 8(a), it can be seen that some particles appeared on the coating and some cracks were generated and extended along with the particles. The cracks were formed during the quick cooling from 1773 K to room temperature. Figure 8(b) displays the cross-section micrograph coating after oxidation for 97 h. The thickness of the coating was about 80 μm while the original thickness was about 200 μm, which indicated that a large amount of the above glassy products was consumed. Figure 8(c) shows the magnification of cross-section micrograph of the coating. The inner layer was SiC and the outer was glassy mixture of ZrSiO₄ and SiO₂. A penetrative crack was found in the coating. During the oxidation, the samples were exposed at 1773 K, the penetrable crack would be self-sealed by SiO₂ glassy mixture to prevent oxidation diffusing (Ref 23). The penetrative crack was formed by the tensile stress when cooled from 1773 K to room temperature. The tensile stress produced may have come from two aspects: one from the thermal expansion coefficient mismatch of the components in the coating, the other one was the crystalline shape change of ZrO₂ (from tetragonal to monoclinic).

4. Conclusions

ZrSiO₄ layer on SiC-C/C composites was obtained by supersonic plasma spraying. It is primarily consisted of ZrSiO₄ and ZrO₂ and exhibited an excellent oxidation protective ability. It could effectively protect the SiC-C/C composites from oxidation over 97 h at 1773 K in the air. The outstanding oxidation protective ability is mainly attributed to the formation of ZrO₂-SiO₂ glassy mixture on the surface of ZrSiO₄ coating.

Acknowledgments

This work has been supported by the National Natural Science Foundation of China under Grant No. 51222207 and 51221001, the Program for New Century Excellent Talents in University, the Research Fund of State Key Laboratory of Solidification Processing (NWPU), China (Grant No. 25-TZ-2009) and “111” Project (Grant No. B08040).

Open Access

This article is distributed under the terms of the Creative Commons Attribution License which permits any use, distribution, and reproduction in any medium, provided the original author(s) and the source are credited.

References

1. T.L. Dhimi, O.P. Bahl, and B.R. Awasthy, Oxidation-Resistant Carbon-Carbon Composites up to 1700 °C, *Carbon*, 1995, **33**(4), p 479-490
2. M.E. Westwood, J.D. Webster, R.J. Day, F.H. Hayes, and R. Taylor, Oxidation Protection for Carbon Fiber Composites, *Carbon*, 1989, **27**(5), p 709-715
3. C.J. Li and A. Crosky, The Effect of Carbon Fabric Treatment on Delamination of 2D-C/C Composites, *Compos. Sci. Technol.*, 2006, **66**(15), p 2633-2638
4. A.S. Ahmed, R.D. Rawlings, S.D. Ellacott, and A.R. Boccaccini, Microstructural and Compositional Characterization of the Pyrocarbon Interlayer in SiC Coated Low Density Carbon/Carbon Composites, *J. Eur. Ceram. Soc.*, 2011, **31**(1-2), p 189-197
5. G.-B. Zheng, H. Sano, and Y. Uchiyama, A Carbon Nanotube-Enhanced SiC Coating for the Oxidation Protection of C/C Composite Materials, *Compos. B Eng.*, 2011, **42**(8), p 2158-2162
6. J.-F. Huang, H.-J. Li, and X.-R. Zeng, Yttrium Silicate Oxidation Protective Coating for SiC Coated Carbon/Carbon Composites, *Ceram. Int.*, 2006, **32**(4), p 417-421
7. Y. Gao, Reaction of ZrO₂-CaO-ZrSiO₄ and ZrO₂-Y₂O₃-ZrSiO₄ Detonation Thermal Sprayed Coatings with Manganese Oxide at 1273 K, *Surf. Coat. Technol.*, 2005, **195**(2-3), p 320-324
8. Q.G. Fu, H. Xue, and H.J. Li, Anti-oxidation Property of a Multilayer Coating for Carbon/Carbon Composites in a Wind Tunnel at 1500 °C, *New Carbon Mater.*, 2010, **25**(4), p 279-284
9. W.-Z. Zhang, Y. Zeng Yi, L. Gologh, X. Xiong, and B.-Y. Huang, Preparation and Oxidation Property of ZrB₂-MoSi₂/SiC Coating on Carbon/Carbon Composites, *Trans. Nonferrous Met. Soc. China*, 2011, **21**(7), p 1538-1544
10. M. Suzuki, S. Sodeoka, and T. Inoue, Zircon-Based Ceramics Composite Coating for Environmental Barrier Coating, *J. Therm. Spray Technol.*, 2007, **17**(3), p 2199-2211
11. J.-F. Huang, X.-R. Zeng, H.-J. Li, X.-B. Xiong, and G.-L. Sun, ZrO₂-SiO₂ Gradient Multilayer Oxidation Protective Coating for SiC Coated Carbon/Carbon Composites, *Surf. Coat. Technol.*, 2005, **190**(2-3), p 255-259
12. Z.H. Han, B.S. Xu, and H.J. Wang, Microstructures, Mechanical Properties and Tribological Behaviors of Cr-Al-N, Cr-Si-N, and Cr-Al-Si-N Coatings by a Hybrid Coating System, *Surf. Coat. Technol.*, 2007, **201**(9-11), p 5223-5227
13. X.C. Zhang, B.S. Xu, and Y.X. Wu, Porosity, Mechanical Properties, Residual Stresses of Supersonic Plasma-Sprayed Ni-Based Alloy Coatings Prepared at Different Powder Feed Rates, *Appl. Surf. Sci.*, 2008, **254**(13), p 3879-3889
14. H. Wu, H.J. Li, and C. Ma, MoSi₂-Based Oxidation Protective Coatings for SiC-Coated Carbon/Carbon Composites Prepared by Supersonic Plasma Spraying, *J. Eur. Ceram. Soc.*, 2010, **30**(15), p 3267-3270
15. G. Di Girolamo, C. Blasi, and L. Pilloni, Microstructural and Thermal Properties of Plasma Sprayed Mullite Coatings, *Ceram. Int.*, 2010, **36**, p 1389-1395
16. H.-J. Li and G.-S. Jiao, Multilayer Oxidation Resistant Coating for SiC Coated Carbon/Carbon Composites at High Temperature, *Mater. Sci. Eng. A*, 2008, **475**, p 279-284
17. T. Fen and H.-J. Li, Microstructure and Anti-oxidation Properties of Multi-composition Ceramic Coatings for Carbon/Carbon Composites, *Ceram. Int.*, 2011, **37**, p 79-84
18. Q.G. Fu, H.J. Li, Y.J. Wang, and K.Z. Li, A Si-SiC Oxidation Protective Coating for Carbon/Carbon Composites Prepared by a Two-Step Pack Cementation, *Ceram. Int.*, 2009, **35**, p 2525-2529
19. T. Aoki, H. Hatta, and T. Hitomi, SiC/C Multi-layered Coating Contributing to the Antioxidation of C/C Composites and the Suppression of Through-Thickness Cracks in the Layer, *Carbon*, 2011, **10**, p 1477-1483
20. Y.C. Zhu, S. Ohtani, and Y. Sato, Formation of a Functionally Gradient (Si₃N₄+SiC)/C Layer for the Oxidation Protection of Carbon-Carbon Composites, *Carbon*, 1999, **37**, p 1417-1423
21. X. Yao, H. Li, and Y. Zhang, A SiC-Si-ZrB₂ Multiphase Oxidation Protective Ceramic, *Ceram. Int.*, 2012, **38**, p 2095-2100
22. A. Kaiser, M. Lobert, and R. Telle, Thermal Stability of Zircon (ZrSiO₄), *J. Eur. Ceram. Soc.*, 2008, **28**, p 2199-2211
23. X.-Y. Yao, H.-J. Li, and Y.-L. Zhang, A SiC/ZrB₂-SiC/SiC Oxidation Resistance Multilayer Coating for Carbon/Carbon Composites, *Corros. Sci.*, 2012, **57**, p 148-153